Simple spectral stray light correction method for array spectroradiometers

Yuqin Zong, Steven W. Brown, B. Carol Johnson, Keith R. Lykke, and Yoshi Ohno

A simple, practical method has been developed to correct a spectroradiometer's response for measurement errors arising from the instrument's spectral stray light. By characterizing the instrument's response to a set of monochromatic laser sources that cover the instrument's spectral range, one obtains a spectral stray light signal distribution matrix that quantifies the magnitude of the spectral stray light signal within the instrument. By use of these data, a spectral stray light correction matrix is derived and the instrument's response can be corrected with a simple matrix multiplication. The method has been implemented and validated with a commercial CCD-array spectrograph. Spectral stray light errors after the correction was applied were reduced by 1–2 orders of magnitude to a level of approximately 10^{-5} for a broadband source measurement, equivalent to less than one count of the 15-bit-resolution instrument. This method is fast enough to be integrated into an instrument's software to perform real-time corrections with minimal effect on acquisition speed. Using instruments that have been corrected for spectral stray light, we expect significant reductions in overall measurement uncertainties in many applications in which spectrometers are commonly used, including radiometry, colorimetry, photometry, and biotechnology.

OCIS codes: 120.6200, 300.6190, 330.1710, 120.5630, 120.280, 120.5240.

1. Introduction

Spectrometers are used in a wide range of applications in the fields of spectroradiometry, spectrophotometry, colorimetry, photometry, and optical spectroscopy. Many of the instruments used in industry are multichannel spectrometers, commonly called array spectrometers or spectrographs, which employ array detectors that can simultaneously acquire an entire spectral image over a finite spectral region. Compared with mechanical-scanning spectrometers, spectrographs can acquire the spectral distribution of a source in a matter of seconds rather than typically minutes.

A spectrograph typically consists of an input optic, an entrance slit, a dispersing element (such as a grating), an array detector, and optics to image the entrance slit onto the array detector (Fig. 1). Because of the inclusion of a dispersing element, the spatial image of the entrance slit falls on different regions of the detector array, depending on its wavelength. Thus a broadband light source forms a spectral image across the detector array. Ideally, an image element on an element of the detector array for a particular field of view and a particular wavelength is composed only of the spectral components of the source element within the particular field of view and within the instrument's bandpass at the particular wavelength. In a practical spectrograph system, however, the image element is modified by the presence of stray or scattered light caused by unwanted imaging and scattering on the optical elements of the instrument (surfaces,[1] mounts, internal baffles, higher-order diffraction, fluorescence, etc.). Stray light can originate from the elements of an extended source inside and outside the instrument's overall field of view and from the spectral components of the particular source element inside and outside the instrument's spectral range. Stray light originating from the elements of an extended source is called spatial stray light and can be described by an instrument's point-spread function. Stray light originating from the spectral components of the particular source element is called spectral stray light and can be described by an instrument's spectral line-spread function (see the definition in Section 2 below). The research reported in this paper focuses on correcting an instrument's response for spectral stray light that is the dominant stray light in many applications.

The authors are with the National Institute of Standards and Technology, 100 Bureau Drive, Gaithersburg, Maryland 20899. Y. Zong's e-mail address is yuqin.zong@nist.gov.

Received 10 June 2005; revised 24 September 2005; accepted 27 September 2005.

0003-6935/06/061111-09$15.00/0

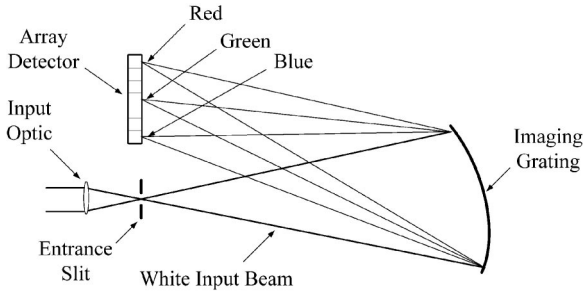

Fig. 1. Illustration of an array spectrometer composed of a fixed imaging grating and a fixed multipixel array detector.

The radiometric performance of spectrographs has improved considerably in recent years, mirroring improvements in array detector technology. However, there is an intrinsic limitation to the measurement uncertainty of a single grating system that is due to the unwanted spectral stray light within the instrument. The level of this spectral stray light is of the order of 10^{-3} to 10^{-5} for the measurement of a monochromatic source or of the order of 10^{-1} to 10^{-3} for the measurement of a broadband source, depending on the quality of a spectrograph. Spectral stray light can cause unexpectedly large errors when one is measuring a low-level spectral component of a broad-band source. For example, a high-quality spectrograph that has a spectral stray light level of 10^{-3} for a broadband source measurement will result in a relative measurement error of 100% of the true value when the spectrograph is used to measure a spectral component that is 0.1% of the averaged signal of the broadband source.

Spectral stray light errors occur in the calibration of the instrument and in subsequent measurements of test sources. Spectroradiometers are typically calibrated against reference standards that utilize incandescent lamps. The peak of the emission from incandescent lamps lies in the red and near-infrared spectral regions. The spectral distribution of the test source often differs significantly from that of the calibration source, in which case the spectral stray light error in the calibration source measurement and that in the test source measurement do not cancel and the errors in the test source measurement are inevitable. In fact, spectral stray light is often the dominant source of uncertainty, particularly when single-grating instruments measure light sources such as light-emitting diodes (LEDs), displays, and some discharge lamps.

Methods were proposed previously to correct spectral stray light errors in spectroradiometers. Kostkowski[2] proposed a spectral stray light correction method for a scanning spectrometer that uses tunable lasers. This method is based on the characterization of a spectrometer's slit scattering function (SSF), which is the relative spectral responsivity when the instrument is set at a fixed wavelength while the wavelength of the incident monochromatic source changes. The SSF of the spectrograph is directly used to obtain the original spectrum by deconvolution to remove the spectral stray light from the total signal by use of an iterative approach. As the responsivity within the bandpass of the spectrograph is several orders higher than that in the out-of-band region, this method requires accurate profiling of the in-band portion of the SSF, which is tedious because the SSF changes rapidly within the bandpass. In practice, the iterative solution may not converge to the correct solution owing to errors in the in-band portion of SSF as well as to measurement noise. Brown *et al.*[3,4] developed a method that solves the convergence problem by separating the SSF into an in-band part and an out-of-band part. Their approach corrects a spectroradiometer's spectral responsivity and a test source's spectral distribution in separate steps. The iterative solution to spectral stray light by this approach is robust and not sensitive to measurement noise or small errors in the derived SSF. In general, extensive fine tuning of the laser, or scanning of the spectrometer's wavelength setting when certain conditions are met,[2] is required for measuring an instrument's SSF accurately.

In this paper we describe a simpler, faster spectral stray light correction method that is based on the ratio of the spectral stray light signal to the total signal within the bandpass of a spectrograph. This functional relationship, set to zero within the bandpass, is called the spectral stray light signal distribution function (SDF). As was done in previous techniques, one first characterizes an instrument by measuring laser emission at a set of wavelengths covering the instrument's spectral range. In the method described here, fine scans of the laser excitation are not needed for calculating the SDFs. A SDF matrix is derived from the characterization measurements and is used to correct the instrument's response for spectral stray light. In contrast to the method of Brown *et al.*, the correction is applied to measured raw output signals, and no distinction is made for the source being measured, *i.e.*, for whether the source is a calibration source or a test source.

The new method corrects for spectral stray light in the system by using a simple matrix multiplication. It is an order of magnitude faster than the iterative approach, and it can be readily incorporated into an instrument's software for real-time correction without affecting the acquisition speed. The method was implemented in a commercial CCD array spectrograph. For experimental validation, several sources were measured and results with and without the spectral stray light correction were compared. The theory of the correction method and the results of the experimental validation are presented.

2. Method of Correction for Spectral Stray Light

An instrument's response to spectral stray light can be characterize by measuring monochromatic spectral line sources that do not have any emission other than the spectral line itself. In this case, the spectral stray light response can easily be separated from the desired signal: Any response measured by array ele-

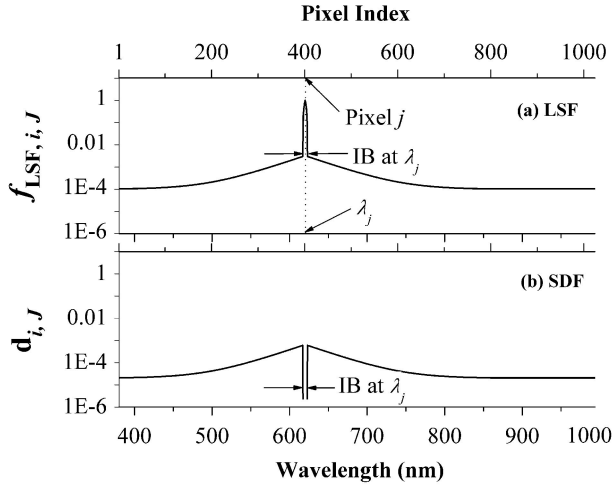

Fig. 2. (a) Illustration of a LSF of a spectrograph with a 1024-pixel array detector. The wavelength of the spectral line source is λ_j, centered on pixel j of the array. (b) Plot of the corresponding SDF derived from the LSF shown in (a). The top x axis is in pixel space, and the bottom x axis is in wavelength space.

ments outside the instrument's bandpass arises from spectral stray light. The excitation source should uniformly fill the instrument's entrance pupil. When the spatial information of the sources is not important (*e.g.*, for spectral radiance of a uniform source or uniform irradiance on a reference plane), the output of a spectrograph using a two-dimensional array detector is usually binned, or integrated, along a column, giving a one-dimensional response. That is, the image of the entrance slit is averaged along an array column, giving one average value per column.

The relationship that describes a spectrograph's relative response at every element i to a fixed monochromatic excitation at wavelength λ_j falling on the element $j = J$ is called the spectral line-spread function (LSF), denoted $f_{\mathrm{LSF}\,i,J}$. The LSF describes the spectral stray light and is conceptually equivalent to the point-spread function that is used to describe the spatial stray light response of an instrument. Figure 2(a) is an illustration of a LSF of a spectrograph that has an array detector with 1024 elements (or pixels). The LSF is normalized by its peak value for convenience. The instrument's response can be separated into a narrow peak region about element j and the remaining broad region of low response. The narrow peak region corresponds to the instrument's bandpass, and the signal in this spectral region is called the in-band (IB) response. The signal in the remaining broad region arises from spectral stray light. Thus the imaging characteristics of the spectrograph can be fully described by use of two indices, i and j; i expresses an output of an individual array element, and j refers to the wavelength, in pixel space, of the incident radiant flux being measured.

The SDF denoted $d_{i,J}$, is derived from the corresponding LSF by normalizing the $f_{\mathrm{LSF}\,i,J}$ to the total IB area and setting values of array elements within the IB area to zero. The SDF generated from the LSF [Fig. 2(a)] is shown in Fig. 2(b). The SDF is given by

$$d_{i,J} = \frac{f_{\mathrm{LSF},i,J}}{\sum_{i\in \mathrm{IB}} f_{\mathrm{LSF},i,J}}, \quad i \notin \text{IB (pixel } i \text{ outside IB)},$$

$$d_{i,J} = 0, \quad i \in \text{IB (pixel } i \text{ inside IB)},$$

$$i = 1 \ldots n. \tag{1}$$

Note that the denominator is simply the sum of the relative signals from the IB elements at each J.

To correct an instrument's response for spectral stray light it is necessary to know the relative stray light response of element i for every excitation wavelength J. This relationship is known as the spectral stray light response function. To generate these spectral relationships it is necessary to know the SDF for every element J in the array. In general, the SDF's of a spectrograph are wavelength dependent; that is, $d_{i,J}$ varies with excitation element J as well. However, it is not required to measure the monochromatic source for $f_{\mathrm{LSF}\,i,J}$ at each element J to obtain a full set of $d_{i,J}$ $(J = 1 \ldots n)$ by using Eq. (1). Because the shape of $d_{i,J}$ typically changes smoothly across the array with excitation element J, $f_{\mathrm{LSF}\,i,J}$ can be measured at intervals much larger than the element interval, and $d_{i,J}$ between the measured excitation elements can be obtained by interpolation or modeling (described below in greater detail).

With $d_{i,J}$ for every excitation element j, the spectral stray light properties of the instrument can be fully characterized. To generate the spectral stray light response function for each element in the array, one forms an $n \times n$ spectral stray signal distribution matrix (SDF matrix) $\mathbf{D}$ by filling the columns of the matrix with the individual SDFs [Eq.(2) below]. That is, each column $j = J$ of $\mathbf{D}$ is filled with a corresponding $d_{i,J}(i = 1 \ldots n)$. From Eqs. (1) the diagonal elements of the matrix and surrounding elements within the instrument's bandpass are 0. Note that each row i in the matrix forms the spectral stray light response function for element $i = I$, $d_{I,j}$ $(j = 1 \ldots n)$:

$$\mathbf{D} = \begin{bmatrix} d_{1,1} & d_{1,2} & \ldots & d_{1,J} & \ldots & d_{1,n-1} & d_{1,n} \\ d_{2,1} & d_{2,2} & \ldots & d_{2,J} & \ldots & d_{2,n-1} & d_{2,n} \\ \vdots & \vdots & \ldots & \vdots & \ldots & \vdots & \vdots \\ d_{i,1} & d_{i,2} & \ldots & d_{i,J} & \ldots & d_{i,n-1} & d_{i,n} \\ \vdots & \vdots & \ldots & \vdots & \ldots & \vdots & \vdots \\ d_{n-1,1} & d_{n-1,2} & \ldots & d_{n-1,J} & \ldots & d_{n-1,n-1} & d_{n-1,n} \\ d_{n,1} & d_{n,2} & \ldots & d_{n,J} & \ldots & d_{n,n-1} & d_{n,n} \end{bmatrix}. \tag{2}$$

Consider the case when a broadband source is measured. The total signal from spectral stray light at a given element i, $y_{\mathrm{s\_spec},i}$ is the sum of all spectral stray light contributions from the broadband source spectra falling on the elements in the array:

$$y_{\mathrm{s\_spec},\,i} = \sum_{j=1}^{n} d_{i,j}\, y_{\mathrm{IB},j,\,\mathrm{true}} \approx \sum_{j=1}^{n} d_{i,j}\, y_{\mathrm{IB},j}, \tag{3}$$

where $y_{\mathrm{IB},j,\mathrm{true}}$ is the true IB signal at element j, which is proportional to the total incident power of the source within the spectral width of element j, and $y_{\mathrm{IB},j}$ is the total IB signal at element j arising from the incident power of the source within the spectral range of IB at element j. $y_{\mathrm{IB},j}$ does not include the signal from element j contributed by spectral stray light and is the unknown variable in Eq. (3).

Note that in Eq. (3) the summation covers only the spectral range of the instrument ($i = 1 \ldots n$). In many cases the spectrum of a measured broadband source extends beyond an instrument's measurable range; in addition, the spectral response ranges of the detector elements are broader than the instrument's spectral range. This is especially true for a spectrograph and can be a problem, for example, when a spectrograph designed for the visible region is calibrated against an incandescent standard lamp whose spectral distribution peaks in the near infrared. In these cases, Eq. (3) does not fully describe the spectral stray light signal, and an additional term δ is required: The expression for the total spectral stray light signal from element i, in these cases, is given by

$$y_{\mathrm{s\_spec},i} = \sum_{j=1}^{n} (d_{i,j}\, y_{\mathrm{IB},j}) + \delta_{\mathrm{spec},i}, \tag{4}$$

where $\delta_{\mathrm{spec},i}$ is the sum of the spectral stray light response of element i to the source emission from outside the instrument's spectral range. The measurement equation for element i is

$$y_{\mathrm{meas},i} = y_{\mathrm{IB},i} + y_{\mathrm{s\_spec},i} = y_{\mathrm{IB},i} + \sum_{j=1}^{n} (d_{i,j}\, y_{\mathrm{IB},j}) + \delta_{\mathrm{spec},i}, \tag{5}$$

where $y_{\mathrm{meas},i}$ is the total measured signal from element i and $y_{\mathrm{IB},i}$ is the IB signal from element i, which is to be obtained as the result of correction. Note that the $\delta_{\mathrm{spec},i}$ component cannot be quantified and corrected with the method described here. However, this component may be negligible or one can reduce it to a negligible level by filtering the radiation entering the spectrograph (see Section 6 below for details). In the following discussion, $\delta_{\mathrm{spec},i}$ is assumed to be zero.

Equation (4) can be expressed in a matrix form, with the spectral stray light signals represented by the column vector $\mathbf{Y}_{\mathrm{s\_spec}}$:

$$\mathbf{Y}_{\mathrm{s\_spec}} = \mathbf{D} \cdot \mathbf{Y}_{\mathrm{IB}}, \tag{6}$$

$\mathbf{Y}_{\mathrm{IB}}$ is a column vector representing the IB signals from the n elements. The measurement equation given as Eq. (5) (with $\delta_{\mathrm{spec},i} = 0$) can also be expressed in matrix form:

$$\mathbf{Y}_{\mathrm{meas}} = \mathbf{Y}_{\mathrm{IB}} + \mathbf{Y}_{\mathrm{s\_spec}} = \mathbf{Y}_{\mathrm{IB}} + \mathbf{D}\mathbf{Y}_{\mathrm{IB}}, \tag{7}$$

where $\mathbf{Y}_{\mathrm{meas}}$ is an n-element column vector with the measured signals.

The matrix measurement equation, Eq. (7), is a system of simultaneous linear equations that has same number of equations as unknowns ($\mathbf{Y}_{\mathrm{IB}}$). It can be rewritten as

$$\mathbf{Y}_{\mathrm{meas}} = [\mathbf{I} + \mathbf{D}]\mathbf{Y}_{\mathrm{IB}} = \mathbf{A}\mathbf{Y}_{\mathrm{IB}}, \tag{8}$$

where $\mathbf{A}(=\mathbf{I} + \mathbf{D})$ is a square coefficient matrix of order n and $\mathbf{I}$ is the $n \times n$ identity matrix. One can obtain each unknown column vector $\mathbf{Y}_{\mathrm{IB}}$ by directly solving Eq. (8), using a proper linear algebraic algorithm (*e.g.*, the Gaussian elimination algorithm). However, in terms of simplicity and calculation speed, it is preferable to solve Eq. (8) by inverting matrix $\mathbf{A}$:

$$\mathbf{Y}_{\mathrm{IB}} = \mathbf{A}^{-1}\, \mathbf{Y}_{\mathrm{meas}} = \mathbf{C}\, \mathbf{Y}_{\mathrm{meas}}. \tag{9}$$

$\mathbf{C}$, the inverse of $\mathbf{A}$, is called the spectral stray light correction matrix. Note that development of matrix $\mathbf{C}$ is required only once, unless the imaging characteristics of the instrument change. Using Eq. (9) enables the spectral stray light correction to become a single matrix multiplication operation, and the correction can be performed in real time with a minimal effect on acquisition speed.

Measurement errors are inevitable and arise from a variety of sources, including errors in coefficients $d_{i,J}$ that are due to errors in the LSFs (both measurement and interpolation), errors in $\mathbf{Y}_{\mathrm{meas}}$ arising from noise, and computational round-off errors. To obtain an accurate solution for $\mathbf{Y}_{\mathrm{IB}}$ by using Eq. (9), it is critical that the solution be numerically stable, that is, insensitive to small errors in the coefficients of matrix $\mathbf{C}$ and in $\mathbf{Y}_{\mathrm{meas}}$. $\mathbf{A}$ is nearly the identity matrix: All diagonal components are 1, with adjacent components all 0 ($d_{i,J} = 0$ inside the defined set of IB elements). The rest of the components in the matrix are typically 3 orders smaller than the diagonal elements (the values of $d_{i,J}$ are typically smaller than 10^{-3}). When $\mathbf{A}$ is nearly the identity matrix, small errors in $\mathbf{D}$, in $\mathbf{Y}_{\mathrm{meas}}$, and in computational round-offs should result in only small errors in the solution, $\mathbf{Y}_{\mathrm{IB}}$.[5]

One can evaluate the numerical stability of a system of simultaneous linear equations mathematically by calculating the condition number,[5] $k(\mathbf{A})$ of the system's square coefficient matrix $\mathbf{A}$. The condition number is a relative error magnification factor of a system of simultaneous linear equations. Changes in either $\mathbf{Y}_{\mathrm{meas}}$ or $\mathbf{A}$ can cause changes $k(\mathbf{A})$ times as large in the solution $\mathbf{Y}_{\mathrm{IB}}$. The condition number of an identity matrix is 1; while the condition number of a singular square matrix is infinite.

In addition to the matrix inversion approach, the matrix measurement equation, Eq. (7), can be solved with the conventional iterative approach by use of the following recursion relation:

$$\mathbf{Y}_{\mathrm{IB}}^{(k+1)} = \mathbf{Y}_{\mathrm{meas}} - \mathbf{D}\mathbf{Y}_{\mathrm{IB}}^{(k)},$$

$$k = 0,\ 1,\ 2,\ \ldots,$$

$$\mathbf{Y}_{\mathrm{IB}}^{(0)} = \mathbf{Y}_{\mathrm{meas}}. \tag{10}$$

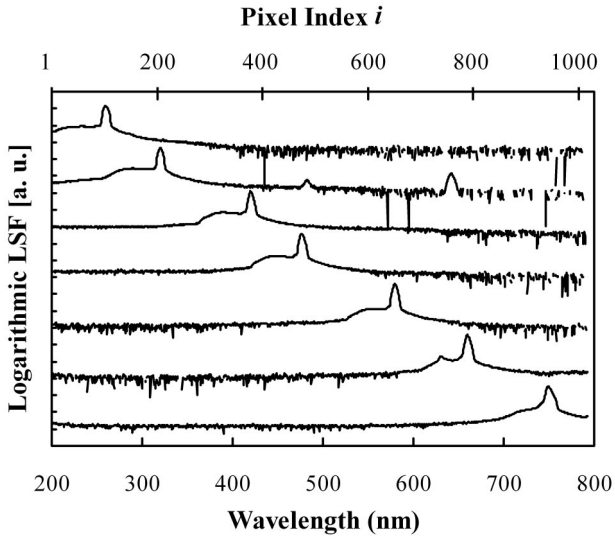

Fig. 3. Representative LSFs spanning the test spectrograph's detector array.

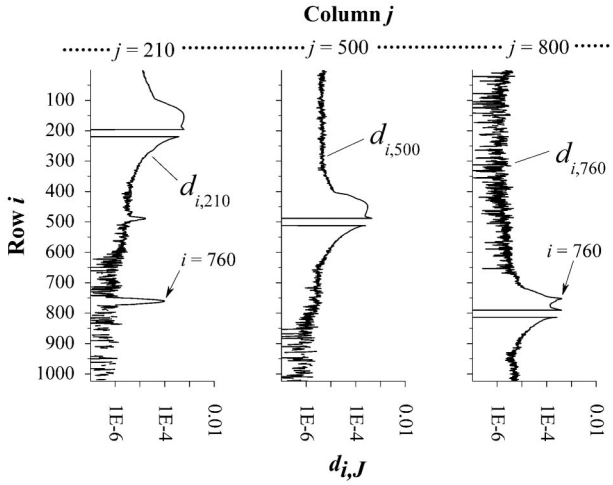

Fig. 4. Three representative columns of the spectrograph's 1024 × 1024 SDF matrix **D**.

The iterative approach is in general slower and more cumbersome than the matrix inversion approach but can be used to validate the matrix inversion approach.

3. Experimental Implementation

A commercial CCD-array spectrograph was corrected for spectral stray light by use of both the spectral stray light correction matrix [matrix **C** in Eq. (9)] and the iterative algorithm [Eq. (10)] to verify the consistency of the two approaches. The spectrometer had a spectral range of 200–800 nm, a pixel-to-pixel spacing of approximately 0.6 nm, and a FWHM bandwidth of approximately 3 nm. The array detector is a two-dimensional CCD with total of 1024 × 128 pixels, the output of which is binned along the column with 128 pixels. The analog-to-digital conversion resolution of the instrument was 15 bits.

Tunable lasers available at the National Institute of Standards and Technology (NIST) Facility for Spectral Irradiance and Radiance Responsivity Calibrations Using Uniform Sources[6] were used for the monochromatic sources that uniformly illuminate the entrance pupil of the spectrograph by using diffusers. For this validation test, the spectrograph measured a total of 80 laser lines with wavelengths spaced as densely as 5 nm (≈8 pixels) apart. The high density of excitation wavelengths ensured that any localized features such as higher-order diffracted light imaged on the array were included in the LSFs. Several representative LSFs spanning the detector array are shown in Fig. 3. The overall spectral stray light signal is fairly low, but there is a large, near-field spectral stray light response (a hump at the immediate left of the IB peaks), which is most likely caused by an interreflection between the CCD array and its detector window. For the UV excitation (≈318 nm, the second curve from the top in Fig. 3), there is an additional small response, peaked at ≈635 nm, arising from the second-order diffraction from the grating. The LSF with a red laser (≈660 nm, the second curve from the bottom in Fig. 3) shows a near-field peak at ≈635 nm, which may result from double diffraction in the spectrograph (a phenomenon in which part of the diffracted light from the grating is reflected back onto the grating and is diffracted a second time).[7]

Each measured LSF, $f_{\mathrm{LSF}\,i,J}$, was used to derive the corresponding SDF, $d_{i,J}$, with Eq. (1). Each derived $d_{i,J}$ filled the corresponding column j of SDF matrix **D.** The intermediate columns between the derived columns were filled by interpolation of the filled known column $d_{i,J}$. The first and last columns were filled by extrapolation. Figure 4 shows logarithmic plots of three representative columns of the spectrograph's 1024 × 1024 SDF matrix **D** for j = 210, 500, 800, which are three SDF functions $d_{i,210}$, $d_{i,500}$, and $d_{i,800}(i = 1 \ldots 1024)$ at the respective excitation pixels J = 210, 500, 800, corresponding to wavelengths of 318, 480, and 660 nm. The curve for column $j = 210(d_{i,210})$, shows a second-order diffraction peak at row i = 760, corresponding to a wavelength of 635 nm. The curve for column j = 800 also shows a near-field peak at row i = 760. Column j = 500 is a typical column SDF of the test spectrograph without any additional features.

Figure 5 shows logarithmic plots of three representative rows of SDF matrix **D** for i = 210, 500, 760, corresponding to wavelengths of 318, 480, and 635 nm. Each curve is a plot of a spectral stray light response function with the excitation pixel changing from 1 to 1024. In the curve for row i = 760 ($d_{760,J}$), there are two peaks, at pixel j = 210 and pixel j = 800. The peak at pixel 210 is due to the second-order diffraction shown in the leftmost curve (j = 210, $d_{i,210}$) in Fig. 4. The small peak at pixel j = 800 is due to the near-field feature shown in the rightmost curve (j = 800, $d_{i,800}$) in Fig. 4.

The condition number, k(**A**), of coefficient matrix **A** [Eq. (8)] of the spectrograph is calculated to be 1.07, very close to the condition number of an identity

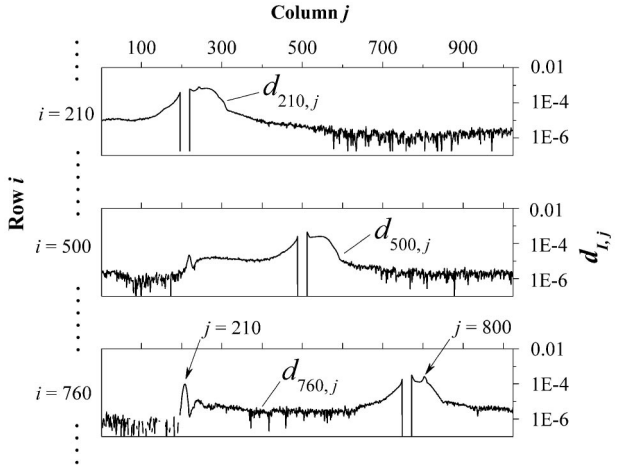

Fig. 5. Three representative rows of SDF matrix **D**.

matrix. This indicates that the solution calculated by the matrix inversion approach is not sensitive to small errors in either the SDF matrix or $\mathbf{Y}_{\text{meas}}$ nor is the solution sensitive to computational round-off errors.

4. Validation Results

We validated the effectiveness of the spectral stray light correction method by measuring broadband sources with the spectrograph. The source uniformly illuminates the entrance pupil of the spectrograph by using diffusers. For each source measurement we averaged 100 readings to possibly evaluate signals lower than one digital count. Figure 6 shows the result of applying the spectral stray light correction to measurements of a broadband source equipped with a bandpass filter. The broadband source was a quartz tungsten halogen lamp with a color temperature of approximately 3100 K. The transmittance of the bandpass filter is lower than 10^{-9} at wavelengths below 420 nm and is lower than 10^{-5} at wavelengths above 770 nm. This condition makes the component,

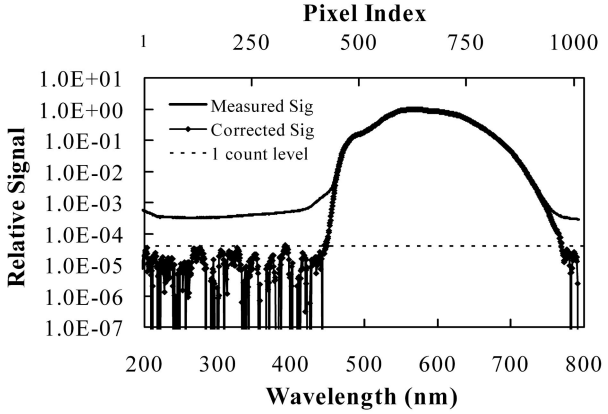

Fig. 6. Result of validation of the spectral stray light correction for a broadband source with a bandpass filter: measured raw signals from the spectrograph, spectral stray light corrected signals, and the one-count level of the 15 bit spectrograph are shown.

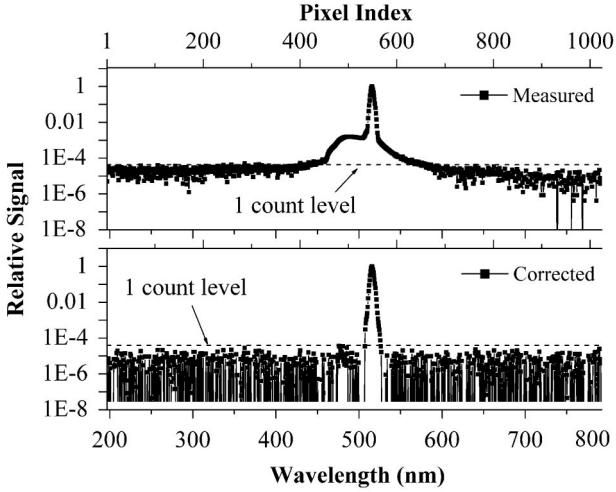

Fig. 7. Result of the spectral stray light correction for a monochromatic laser source at 516 nm. Measured raw signals from the spectrograph, spectral stray light-corrected signals, and the one-count level of the 15-bit spectrograph are shown.

$\delta_{\text{spec},i}$, which would otherwise be present in this instrument, negligible when one is measuring a quartz tungsten halogen lamp. As shown in Fig. 6, the original relative spectral stray light signals were approximately 5×10^{-4} of the maximum value at wavelengths below 400 nm and above 770 nm. After the correction, the relative spectral stray light signals were reduced by more than 1 order of magnitude, to a level of approximately 10^{-5}, equivalent to less than one count of the 15-bit spectrograph. Similar results of spectral stray light signal reduction were obtained when the quartz tungsten halogen lamp with other bandpass filters was measured.

The effectiveness of the spectral stray light correction method for measurements of narrowband sources was also evaluated. As an extreme example of a narrowband source, a 516 nm monochromatic laser source was measured. The laser source was not one of the selected lasers used to characterize the spectrograph for spectral stray light. Figure 7 shows that the instrument response that is due to spectral stray light was corrected to a level equivalent to less than one count of the 15-bit spectrograph, or to a level well below 10^{-5} in most of the spectral region. The interreflection peak (the hump at the left side of the IB peak) was also eliminated.

Both the spectral stray light correction matrix [matrix **C** in Eq. (9)] and the iterative algorithm [Eq. (10)] were used to correct the spectral stray light errors in measured signals in the two measurements for the broadband and the narrowband sources described above. The iterative algorithm converged to a stable solution within three iterations. Both solutions were robust; small changes in the measured signals, arising from noise, for example, produced only small changes in the solution. No noticeable differences between the results from the two approaches were observed. The solution based on spectral stray light correction matrix **C** gives the same results as the

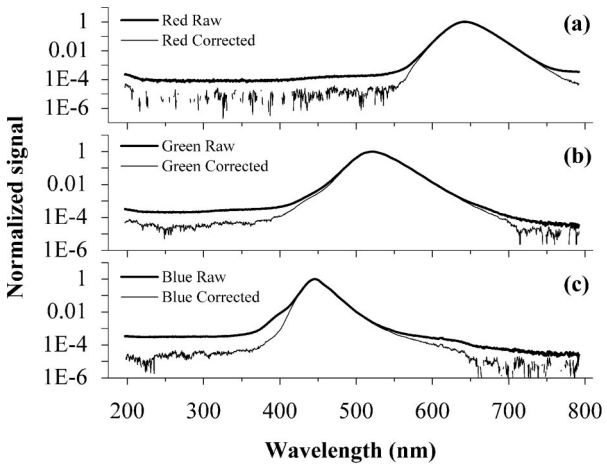

Fig. 8. Plots of the raw and the spectral stray light corrected signals of the three LEDs, normalized to the respective raw peak signals: red, green, and blue LEDs are shown. Thicker curves, measured relative spectral signal distribution; thinner curves, spectral stray light corrected spectral signal distribution.

iterative algorithm, but the calculation is an order of magnitude faster.

5. Spectral Stray Light Correction Example

The spectrograph was used to measure three LEDs (red, green, and blue). In these measurements the incident flux outside the spectral range of the spectrograph are negligible, thereby approximating $\delta_{\text{spec},\,i} \approx 0$. Figure 8 shows logarithmic plots of the raw and the spectral stray light corrected signals of the three LEDs, normalized to the respective raw peak signals. Below 400 nm, where the radiant flux from the LEDs is negligible, the corrected values of all three LEDs were reduced by approximately an order of magnitude. The correction on the right-hand side of the peak wavelength varies with individual LEDs because of their different spectral distributions.

6. Discussion

Typical spectrographs have pixel-to-pixel intervals much smaller than the bandwidth; thus there are several pixels within a bandpass. If the bandwidth is not large, only a few pixels cover the bandpass, in which case the shape of the IB part of the LSF (narrow peak part) depends strongly on where the laser line falls with respect to a pixel's peak responsivity. However, the sum of the IB pixel signals will be fairly constant as long as each array pixel has reasonably uniform responsivity over the light-sensitive area (several percent typically) and the dead areas between pixels are small compared with the pixel size (this is true for most CCD and photodiode arrays). We verified the test spectrograph for insensitivity of the IB signal to the laser wavelength by scanning a tunable laser in wavelength across two adjacent pixels. No meaningful change in the total IB signal was observed, as expected. This insensitivity of the SDF to laser wavelengths eliminates the need for fine tuning of the laser, which is time consuming, to characterize the instrument's LSFs and enables the characterization to be done by use of a set of fixed-wavelength lasers if available.

Knowing the bandwidth of the monochromatic radiation is not critical for this method because the LSF is normalized simply by the sum of the signals from the IB pixels. Thus a variety of lasers with finite bandwidth (e.g., quasi-cw UV lasers and diode lasers) can be used. In principle, another source, such as a discharge-lamp-based line source, an optical filter based line source, a double-monochromator based tunable source, or a tunable filter based source, could also be used as long as the source has negligibly small out-of-band emission and sufficient power to allow measurements to be made with large signal-to-noise ratios.

It is important that the instrument have enough signal dynamic range and sensitivity that the LSF can be measured accurately. This typically requires that an instrument have 15 bits of resolution in its analog-to-digital converter, which is common nowadays. For a spectrograph that does not have enough signal dynamic range, or a spectrograph for which the spectral stray light signal is too low for a monochromatic source to be used, one may obtain the LSF with high resolution by using what is called the bracketing technique, in which a spectrum is measured with a set of different integration times, allowing the low-level part of the spectrum to be measured with high resolution (with the peak region saturated), and the measured spectrum data are assembled to generate a spectrum with a larger dynamic range. One might also obtain a high-resolution LSF by measuring the monochromatic source at different power levels and then combining the results; this may result in saturation of the IB signal for the higher power levels.

SDF matrix **D** of a spectrograph is derived from the measured LSFs, which are relative functions. Thus, in principle, SDF matrix **D** is stable after the system is constructed, especially for the spectrographs that are completely sealed after the entrance slit. The LSFs of spectrographs have been measured over a period longer than 5 years without showing any measurable changes.[8] Therefore, while periodic checks of the LSFs are important, full characterizations on a yearly schedule are not needed. However, it should be noted that any configuration change of the spectrograph is likely to cause changes in the LSFs, in which case the LSF needs to be remeasured. For example, changing input optics to measure radiance instead of irradiance can change the spectral stray light characteristics in the spectrograph. In principle the changes are small, and one can monitor changes in the LSFs by measuring a few monochromatic sources.

Off-array additional spectral stray light signal term $\delta_{\text{spec},i}$ must be close to 0 for effective correction. When a source has significant power outside the instrument's designed spectral range, uncorrected spectral stray light signal $\delta_{\text{spec},\,i}$ can be significant. In particular, the measurement error tends to be significant when an instrument (designed for the UV and visible regions) is calibrated with an incandescent

lamp and is used to measure a blue or UV source. In this case, $\delta_{\mathrm{spec},i}$ may be large for the calibration measurements because the array detectors typically have much lower spectral responsivity in the blue or UV region than in the near-IR region and because incandescent lamps typically have a peak power in the near IR region. As off-array radiant flux does not follow the normal optical path, it is difficult to model and quantify its contribution to the total spectral stray light signal, and there is no way to determine the magnitude of the IR flux. The best solution is to block the incident flux that lies in spectral regions outside the instrument's designed spectral range by using a proper optical filter. The condition $\delta_{\mathrm{spec},i} \approx 0$ is already satisfied if a spectrograph's designed operational range is matched to the spectral response of the array detector, e.g., when silicon photodiodes are used for the array detector and the instrument's spectral range coverage is as much as 1100 nm. In this case the array detector does not respond to radiation beyond the long-wavelength limit, and the flux below the short-wavelength limit is typically small.

Theoretically, one can also apply this method to scanning-type spectrometers by replacing the pixels with the scanning positions of the spectrometer. In this case it is required that the spectrometer scan in a wavelength interval that matches its bandwidth, or scan with an interval that is a fraction of its bandwidth, to ensure the insensitivity of the integrated IB signal to small offsets in laser wavelength.[9] The principle developed for this spectral stray light correction method can also be used to correct additional measurement errors resulting from different mechanisms (as demonstrated by correction of second-order diffraction signals). One example is the correction of measurement errors that are due to fluorescence of optical materials in a measurement system. Signals from fluorescence can be treated in the same way as the spectrometer's spectral stray light signal and can be corrected with this method. Such a correction for fluorescence errors was applied successfully to an integrating sphere-spectrograph system at NIST.[10]

7. Conclusions

A simple, effective method to correct a spectrometer's output signals for spectral stray light errors has been developed based on the characterization of the instrument's response to monochromatic radiation at a set of wavelengths. This method does not require fine tuning of the wavelength of monochromatic radiation, and thus, in principle fixed-wavelength spectral line sources can also be used. Once characterized, the spectral stray light contributions to the raw output signals of the spectrometer can be corrected with a simple matrix multiplication by use of the spectral stray light correction matrix. This fast spectral stray light correction matrix approach can easily be implemented in an instrument's software for real-time corrections with minimal degradation in acquisition speed.

The method has been implemented and tested by use of monochromatic tunable laser sources and a CCD-array spectrometer. Validation results demonstrate that, by using the spectral stray light correction method, one can reduce the magnitude of the spectral stray light signal in a spectrograph by 1–2 orders of magnitude, to a level of 10^{-5} or lower for a source measurement, equivalent to less than one count of the 15-bit instrument. It is critically important that the off-array radiation in the spectrometer be blocked to achieve an extremely low spectral stray light level after correction.

This method can also be extended to correct spectral stray light errors of scanning-type spectrometers. The principle can be used to correct other types of error resulting from different mechanisms, for example, fluorescence of optical materials used in a spectrometer system. We are also extending this technique to correct stray light errors in hyperspectral imaging instruments, which includes the correction of both spectral and spatial stray light.

Correcting spectroradiometers for spectral stray light within the system should yield significant reductions in overall measurement uncertainties in radiometry, photometry, colorimetry, biotechnology, and other areas for which these instruments are commonly used. We are examining the efficacy of transferring the SDF matrix from one instrument that has been extensively characterized to a second instrument with a similar design by using a limited laser data set. If this procedure is successful, it will enable a correction matrix to be developed for an entire spectrograph model, making its implementation cost effective, thereby facilitating widespread dissemination of the approach.

The authors thank Albert C. Parr and C. Cameron Miller of the NIST Optical Technology Division, Dennis K. Clark of the National Oceanic and Atmospheric Administration, James L. Mueller of the Center for Hydro-Optics and Remote Sensing, Richard Distl of Instrument Systems GmbH, Richard Young of Optronic Laboratories, Inc., Scott D. McLean of Satlantic, Inc., and David Gross of Osram Sylvania, Inc., for helpful discussions of the spectral stray light characteristics of array spectrometers.

References

1. T. N. Woods R.T Wrigley III, G. J. Rottman, and R. E. Haring, "Scattered light properties of diffraction gratings," Appl. Opt. **33,** 4273–4285 (1994).
2. H. J. Kostkowski, ed., "Spectral scattering," in *Reliable Spectroradiometry* (Spectroradiometry Consulting, La Plata, Md., 1997), pp. 57–87.
3. S. W. Brown, B. C. Johnson, M. E. Feinholz, M. A. Yarbrough, S. J. Flora, K. R. Lykke, and D. K. Clark, "Stray light correction algorithm for spectrographs," Metrologia **40,** S81–83 (2003).
4. S. W. Brown, D. K. Clark, B. C. Johnson, H. Yoon, K. R. Lykke, S. J. Flora, M. E. Feinholz, N. Souaidia, C. Pietras, T. C. Stone, M. A. Yarbrough, Y. S. Kim, R. A. Barnes, and J. L. Mueller, "Advances in radiometry for ocean color," Chap. 7 *of Special Topics in Ocean Optics Protocols,* Part 2 of Ocean Optics Protocols for Satellite Ocean Color Sensor Validation, Rev. 5, Vol. VI, J. L. Mueller, G. S. Fargion, and C. R. McClain, eds. (NASA Goddard Space Flight Center, 2004), pp. 8–35.

5. C. B. Moler, ed., "Linear equations," in *Numerical Computing with Matlab* (Society for Industrial and Applied Mathematics, 2004), pp. 53–92.
6. S. W. Brown, G. P. Eppeldauer, and K. R. Lykke, "NIST facility for spectral irradiance and radiance responsivity calibrations with uniform sources," Metrologia **37,** 579–582 (2000).
7. Richard Young, Optronic Laboratories, Inc., 4632 36th Street, Orlando, Fla. 32811 (personal communication, 2004).
8. Dennis K. Clark, National Oceanic and Atmospheric Administration, NOAA/NESDIS, 5200 Auth Rd., Camp Springs, MD 20746 (personal communication, 2004).
9. CIE Technical Committee 1–48, "Recommendations concerning the calculation of tristimulus values and chromaticity coordinates," in *Colorimetry*, CIE Tech. Rep. CIE 15:2004, 3rd ed. (Commission Internationale de l'Eclairage, 2004), pp. 12–16.
10. Y. Zong, C. C. Miller, K. R. Lykke, and Y. Ohno, "Measurement of total radiant flux of UV LEDs," in *Proceedings of the CIE Symposium '04, LED Light Sources: Physical Measurement and Visual and Photobiological Assessment,* CIE publ. x026:2004 (Commission Internationale de l'Eclairage, 2004), pp. 107–110.